参考著作No.9

Proceedings of the Institution of Civil Engineers - Structures and Buildings

ISSN 0965-0911 | **E-ISSN** 1751-7702

Volume 171 Issue 7, July, 2018, pp. 517-527

< Prev Next >

Probabilistic safety evaluation of a river bridge substructure against floods

Authors: Kuo-Wei Liao, PhD Wan-Chien Kung, MSc Jyun-Wei Chen, MSc

Cite this article
Liao KW, Kung WC and Chen JW (2018)
Probabilistic safety evaluation of a river bridge substructure against floods.
Proceedings of the Institution of Civil Engineers – Structures and Buildings **171(7)**: 517–527,
https://doi.org/10.1680/jstbu.16.00028

Research Article
Paper 1600028
Received 06/02/2016;
Accepted 24/08/2017;
Published online 17/10/2017

Keywords: floods & floodworks/
risk & probability analysis/
river engineering

参考著作No.9

Structures and Buildings

ice publishing

Probabilistic safety evaluation of a river bridge substructure against floods

1 Kuo-Wei Liao PhD
Associate Professor, Department of Bioenvironmental Systems Engineering, National Taiwan University, Taipei, Taiwan (corresponding author: kliao@ntu.edu.tw)

2 Wan-Chien Kung MSc
Graduate student, Department of Civil Engineering, National Taiwan University, Taipei, Taiwan

3 Jyun-Wei Chen MSc
Graduate student, Department of Civil & Construction Engineering, National Taiwan University of Science & Technology, Taipei, Taiwan



Many factors affect the safety of a reinforced concrete river bridge, and some of these factors might have significant uncertainty that should be evaluated. This study focuses on a system reliability analysis of a reinforced concrete bridge, which is the most common type of river bridge in Taiwan. Specifically, non-linear behaviours of core/cover concrete and steel reinforcement in the substructure of a bridge are considered. Uncertainties of stream surface elevation, water velocity, local scour depth, soil property and record-to-record variations are included in the probabilistic model. The aforementioned parameters of six river geometries are incorporated into a Hydrologic Engineering Center-river analysis system (HEC-RAS) model to assess their impacts on the bridge safety. The effect of river geometry has not been studied thoroughly. Results shown here indicate that it plays an important role. Adopting Bayesian theory to consider the record-to-record uncertainty by combining historic and HEC simulation data is another innovative aspect of this study. Monte Carlo simulation is used to conduct the reliability analysis. The results obtained indicate that the proposed procedure for the bridge reliability analysis is consistent with expert engineering judgement and that the variation in scouring depth and river geometry are pertinent to bridge safety.

Notation

A_b	area of pile bottom
A_s	pile surface area
D	pile diameter (m)
D_f	failure domain
E	elastic modulus (tf/m^2)
E_c	tangent modulus of elasticity of the concrete (MPa)
E_{sec}	secant modulus of elasticity
f_s	friction resistance pressure on surface of pile
f_1, f_2, f_3, f_4, f_5	performance functions
$f_X(x)$	probability distribution function
f'_{cc}	compressive strength of the confined concrete
f'_{co}	unconfined concrete compressive strength
$f'(\theta)$	prior probability derived from the existing reports
$f''(\theta)$	posterior probability
h_0	interim factor in Chang's formula
I	pile cross-sectional moment of inertia (m^4)
K_2	short-term loading cases
K_3	long-term loading cases
k	horizontal subgrade reaction coefficient (tf/m^3)
$L(\theta)$	likelihood function
M_t	applied bending moment on pile head
$N_\mu(x_i, \sigma)$	Gaussian density function of μ with mean value x_i and standard deviation (σ)
$n \times m$	total number of piles
P	applied vertical load
P_f	probability of failure
$P(\varepsilon\|\theta)$	likelihood of simulation outcome ε assuming a given θ
q_b	allowable vertical pressure at pile bottom
r	interim factor in Mander's approach
$\hat{\mu}$	Bayesian estimator for the mean values or standard deviations of the water surface elevation and water velocity
V_c	nominal shear strength provided by concrete
V_n	total nominal shear strength
V_s	nominal shear strength provided by shear reinforcement
V_t	applied shear force on top of pile
w_p	pile weight
x	distance between the measured point to top of the river bed
$\bar{x}$	sample mean
β	reliability index

ε_c	longitudinal compressive concrete strain
ε_{cc}	strain corresponding to the maximum concrete stress
ε_{co}	strain corresponding to unconfined concrete strength
Λ	interium factor in Chang's formula
μ	target parameter
σ	resulting stress of outermost pile due to bending moment
σ_y	yielding stress
τ_y	shear strength of the pile

1. Introduction

A bridge is a structure that crosses a physical barrier without interrupting the functions of the object it passes over, such as a body of water, valley, or road. If a bridge is over a river (i.e. a body of water), it is referred to as a river bridge in this study. To be specific, only bridge foundations located within a river are considered in this study. Many factors affect the safety of a river bridge during floods. Because of the large number of important factors, it is not easy to perform a bridge safety evaluation, even using a deterministic approach. For example, a preliminary inspection using examination by eye in Taiwan identified 13 such factors, including upstream river dam or reservoir facilities, foundation type, location of bending or narrowing of the river, eroded river bed, material of the river bed, location of the main channel, hydraulic drop effect, flow attack angle, area ratio of the bridge to its cross-section, foundation scouring depth, effective pier diameter, protection of the river bank and protection of the river bed (Liao *et al*., 2015). A comprehensive analysis that includes all of these factors is obviously complicated. Nonetheless, it is important to develop a reasonable solution to help the engineers responsible to ensure bridge safety. Among these 13 items, the bridge strength was identified as playing an important role in the overall evaluation. Specifically, the weight of all items related to the bridge structure – including foundation type, location of the main channel, flow attack angle, area ratio of the bridge to its cross-section, foundation scouring depth and effective pier diameter – accounts for 57 out of 100. Moreover, in Taiwan, a levee protection system for a river bank is often used to prevent a bridge collapse due to river channel instability. If the river channel stability is included, the overall weight increases from 57 to 72. Thus, this study proposes to evaluate bridge safety by analysing the bridge structure and the parameters related to it and river channel stability.

In addition to the complicated process in a deterministic analysis, the process of bridge safety evaluation involves assessment of a large number of uncertainties. Taking the river channel stability as an example, a stable river channel is an ideal situation. However, this is not true for the majority of the rivers in Taiwan. To consider the effect of river instability, six recorded cross-geometries of river channels are selected for analysis. Another example of uncertainty is a distinguishable variation found in water surface elevation and velocity due to variations in the geometry of the river section, Manning's coefficient and the analysed model (e.g. US Army Corps of Engineers Hydrologic Engineering Center-river analysis system (HEC-RAS)). Thus, proper evaluation of bridge safety requires a rigorous probabilistic approach, which has been utilised in several earlier studies. Johnson *et al*. (2015) quantified uncertainties in parameters such as bridge pier, abutment and contraction scour based on the analysis of available laboratory data. They used several scour equations as the basis for their uncertainty studies. The bridge reliability was then evaluated based on these equations and their corresponding uncertainties. Davis-McDaniel *et al*. (2013) proposed a process for failure risk analysis for bridges in South Carolina, USA using fault-tree modelling. They found that the top five critical factors that led to a bridge failure were flood, scour, overloading, corrosion of post-tensioning tendons and earthquakes. Saydam *et al*. (2013) also applied a reliability-based approach to compute component and system failure probabilities of bridge superstructures in Wisconsin, USA.

A system reliability analysis consisting of five limit states is used in the proposed bridge safety evaluation. In general, most probable point (MPP)-based reliability analysis methods (e.g. first-order reliability method (Form)) are not suitable for a system reliability analysis. Therefore, this study has adopted Monte Carlo simulation (MCS) to solve bridge reliability. MCS regards reliability analysis as an integral problem

$$1. \quad P_f = J = \int \cdots \int_{D_f} f_X(x)\mathrm{d}x$$

where P_f is the probability of failure, D_f is the failure domain, and $f_X(x)$ is the probability distribution function of the performance function. It is recognised that MCS does not offer any advantages in terms of computational cost. However, in Taiwan, bridges are usually designed for a 100 year flood, and thus, the resulting failure probability is often not a small number. For this reason, the computational cost of MCS is affordable and is adopted here. The five performance functions considered are the soil bearing capacity, the soil resistance to a pulling force, the pile shear strength, the pile axial strength and the bridge serviceability (the top displacement of a pile). A flowchart of the overall analysis process is provided in Figure 1.

2. Description of performance functions

According to the *The Bridge Design Specifications* (MOTC, 2009), the performance function of the soil bearing performance is

$$2. \quad f_1 = A_s f_s + A_b q_b - \frac{P}{n \times m} - \sigma A$$

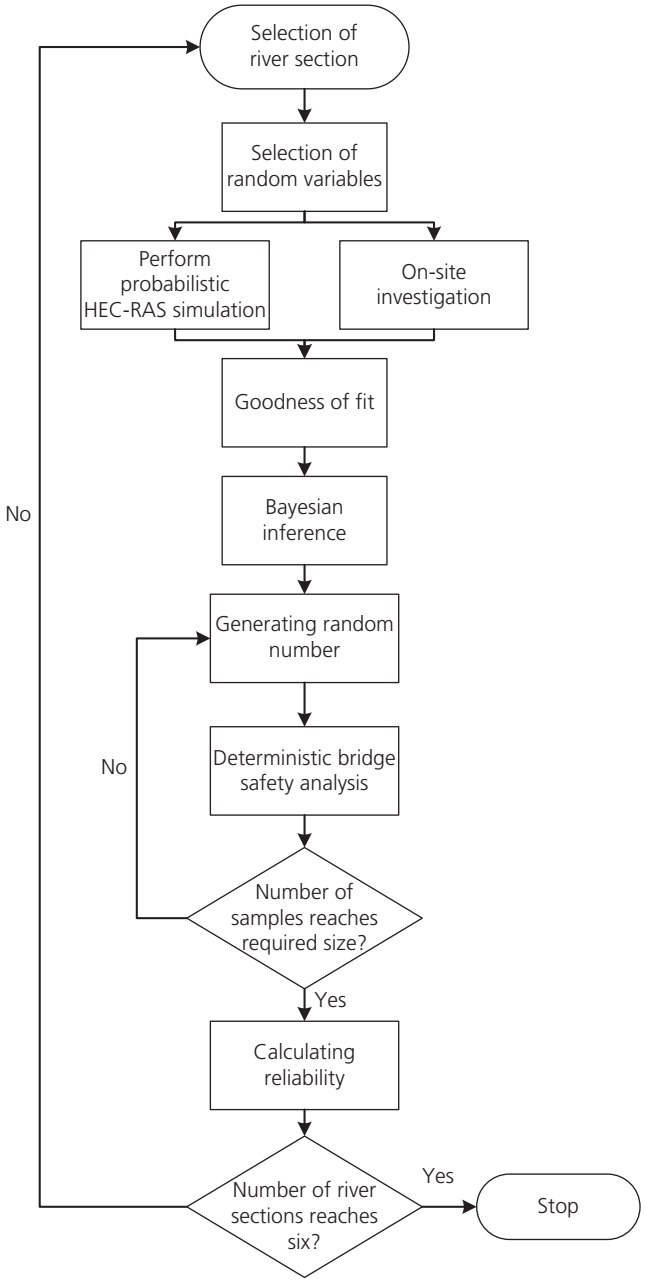

Figure 1. A flowchart for the overall analysis

where A_s is the pile surface area; f_s is the friction resistance pressure on the surface of the pile; A_b is the area of the pile bottom; q_b is the allowable vertical pressure at the pile bottom; P is the applied vertical load; $n \times m$ is the total number of piles; σ is the resulting stress of the outermost pile due to the bending moment; and A is the pile area. The performance function of the soil pulling force is

$$3. \quad f_2 = w_p + \frac{1}{K_2} A_s f_s + \frac{P}{n \times m} - \sigma A$$

where w_p is the pile weight, and K_2 is 3 for the short-term loading case and 6 for the long-term loading case (according to *The Bridge Design Specifications* (MOTC, 2009)).

The capacity of the pile strength is calculated by multiplying the material strength by the corresponding sectional area. The demand of the pile strength is computed using the equations provided by Chang's simplified lateral pile analysis (Chang and Chou, 1989). Chang and Chou (1989) categorised the pile foundations into six types depending on their boundary conditions. The performance functions of the pile shear stress, the pile axial stress and the bridge serviceability (the horizontal displacement on the pile head) can be described by Equations 4, 5 and 6, respectively.

$$4. \quad f_3 = A\tau_y - V_t e^{-\lambda x}[\cos(\lambda x) - (1 + 2\lambda h_0)\sin(\lambda x)] = 0$$

$$5. \quad f_4 = \frac{I\sigma_y}{y} - \frac{V_t}{\lambda} e^{-\lambda x}[\lambda h_0 \cos(\lambda x) + (1 + \lambda h_0)\sin(\lambda x)]$$

$$6. \quad f_5 = 1{\cdot}5 - 0{\cdot}01\left(\frac{V_t}{2EI\lambda^3} + \frac{M_t}{2EI\lambda^2}\right)$$

where τ_y is the shear strength of the pile; V_t is the applied shear force on the top of the pile (tf); $\lambda = [(kD/EI)^{1/2}]^4$ (m^{-1}); k is the horizontal subgrade reaction coefficient (tf/m^3); D is the pile diameter (m); E is the elastic modulus (tf/m^2); I is the pile cross-sectional moment of inertia (m^4); x is the distance from the measured point to the top of the river bed; $h_0 = M_t/V_t$ (m); σ_y is the yielding stress; 1·5 (cm) is the displacement capacity; and M_t is the applied bending moment on the pile head. V_t and M_t (in Equations 4–6) are affected by the flexural and shear behaviours of the pier described in Section 3. Please note that according to Chang's approach, there are two boundary conditions for the pile head: free or restrained. The boundary condition of the pile head depends on the stiffness of the pile cap. Based on the building foundation design specifications in Taiwan (CPAMI, 2001), if the thickness of the pile cap is less than the pile diameter, then the deformation effect of the pile cap should be considered and is assumed to be free in the current study. However, if the thickness of the pile cap is greater than the pile diameter, then the pile head is assumed to be restrained. For example, if the pile cap is categorised as a fixed end, the pile head displacement can be computed using Equation 6.

3. Modelling of the reinforced concrete pier

The pier ends may form a plastic hinge and can be described by the combination of flexural and shear behaviours (Sung *et al.*, 2005). Using the stress–strain curves of concrete and steel together with a moment–curvature analysis, the pier flexural behaviour can be determined. The concrete model proposed by Mander *et al.* (1988) is adopted. In this model, the

longitudinal compressive concrete stress (f_c) of the confined concrete is described by

$$f_c = \frac{f'_{cc} x r}{r - 1 + x^r} \quad (7)$$

where f'_{cc} is the compressive strength of the confined concrete and x is calculated by

$$x = \frac{\varepsilon_c}{\varepsilon_{cc}} \quad (8)$$

where ε_c is the longitudinal compressive concrete strain. ε_{cc} is calculated by

$$\varepsilon_{cc} = \varepsilon_{co}\left[1 + 5\left(\frac{f'_{cc}}{f'_{co}} - 1\right)\right] \quad (9)$$

where ε_{co} is equal to 0·002 and f'_{co} is the unconfined concrete compressive strength. The value of r in Equation 7 is calculated by

$$r = \frac{E_c}{E_c - E_{sec}} \quad (10)$$

where $E_c = 5000(f'_{co})^{1/2}$ MPa is the tangent modulus of elasticity of the concrete and

$$E_{sec} = \frac{f'_{cc}}{\varepsilon_{cc}} \quad (11)$$

A similar approach is applied to the cover concrete, details can be found in Mander *et al.* (1988).

The shear behaviour of a pier is built using the stress–strain curves and Equation 12

$$V_n = V_c + V_s \quad (12)$$

Please note that V_n is a function of rotation (θ) and can be transformed to the corresponding bending plot (from $V_n - \theta$ to $M - \theta$). The combination of flexural and shear behaviours are used to describe the pier plastic formulation. If any plastic hinge formed, the stress will be redistributed resulting to different values of V_t and M_t (in Equations 4–6).

4. Uncertainties considered in the current studies

4.1 Random variables

The five random variables (as shown in Figure 2) considered here are water surface elevation, water velocity, local scour depth, wind load and soil property. Initial values of the water surface elevation and velocity were determined by a hydraulic analysis of different discharge rates at the upstream area. Then, the obtained values were updated using Bayesian theory to account for the record-to-record uncertainty. Local scour depth can be determined using an empirical equation that is a function of water surface elevation and velocity. Among many available empirical equations, it is not easy to verify which equation is the most appropriate formula for the specified bridge. In this case, several suggested equations from earlier studies are used. This assumption results in a large uncertainty known as the modelling error (i.e. epistemic uncertainty) in the analysis process. Details of random variables considered here are provided below.

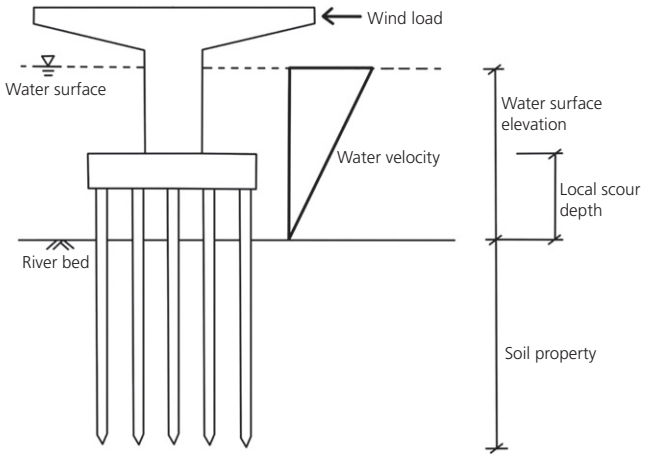

Figure 2. Illustration of random variables considered in the current study

4.1.1 Water velocity and water surface elevation

The mean values of the water surface elevation and velocity are determined later using Equation 19. Details are described in Section 4.2. The current section focuses on the distribution types and variations determined based on the simulation results of HEC-RAS. Two random variables, the discharge rate and Manning's roughness coefficient, are considered in the HEC-RAS simulation.

Earlier records (WRAMOEA, 2011b) show that the Manning's roughness coefficient for the Dajia River basin is between 0·02 and 0·045. Because no further information could be found, a uniform distribution with the bounds provided in the literature is assumed for Manning's coefficient. The overflow hydrograph collected in the upstream dam is used as the input for the HEC-RAS model. Figure 3 displays an example of the outflow hydrograph at the Ma-An dam during typhoon Gu-Chou. It is expected that some of the collected outflow hydrographs might not be statistically consistent with the rest of the data. A statistical method, the modified Thompson τ technique, is used here to decide whether to retain or discard the suspected outliers.

Based on the HEC-RAS simulation results, a chi-square test is used to determine the probability density function (pdf) for

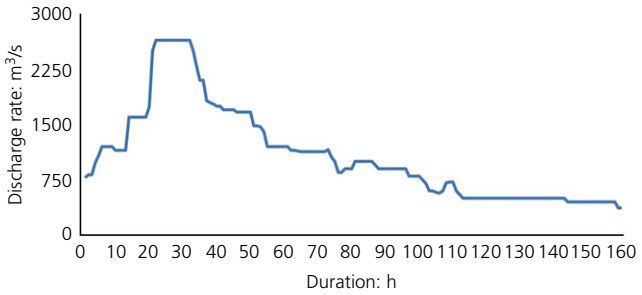

Figure 3. Outflow hydrograph at the Ma-An dam during typhoon Gu-Chou

Table 1. *P*-values for different pdfs (2012)

	Stream level	Water velocity
Normal	0·45	0·80
Log-normal	0·57	0·25
Extreme	0·08	0·65
Exponential	~0·00	~0·00
Rayleigh	~0·00	~0·00
Weibull	0·42	0·82

the water surface elevation and water velocity. The test results are displayed in Table 1. It can be seen that many pdfs are suitable for describing the randomness of water surface elevation and velocity if the usual significance level (5%) of the *p*-value is used. The Gaussian is selected to be consistent with the formula used in Section 4.2. The standard deviations (STDs) of the water surface elevation and velocity are determined using the samples from the HEC-RAS simulations.

4.1.2 Local scour depth

Many formulas have been proposed for calculating the local scour depth. For example, nine formulas were suggested by Liao *et al.* (2015), and they are adopted here. Using these nine formulas and 30 pairs of the water surface levels and water velocities obtained in Section 4.1.1, 270 samples of the scour depth are obtained. The sample mean is used as the population mean in the following reliability analysis, and one-sixth of the difference between the maximum and minimum calculated depths is assumed to be the STD. This assumes that the scour depth used in the following reliability analysis has an approximate probability of being located within the range estimated by the formula of 99·73%. The overall scour depth of a pier is often equal to the sum of the local scouring, contraction scouring and general scouring (i.e. scouring without structures). For the bridge site investigated here, the local scouring is a dominant parameter, and thus, other types of scouring are not considered in this study.

4.1.3 SPT-*N* values and wind load

The distribution of the standard penetration test blow-count value, SPT-*N*, is summarised according to the geological reports (MOTC, 2004) by the Ministry of Transportation in Taiwan as described below.

(*a*) The first stratum (immediately below the river bed): the thickness is approximately 3·1 m, and the SPT-*N* value has the approximate range of 7–15.
(*b*) The SPT-*N* value of the soil strata below the first stratum is approximately 50.

The SPT-*N* values in the first stratum are assumed to follow the uniform distribution that has the upper and lower bounds indicated above. A deterministic SPT-*N* value of 50 is assigned for the second stratum.

Regarding the wind load, the force on the bridge is calculated by multiplying the wind-induced pressure and its corresponding area affected by the water surface level. Once the water surface level has been determined as described in Section 4.1.1, the projected area of the wind loads can be obtained.

4.2 Consideration of record-to-record uncertainty using Bayesian theory

This section provides information for determining the mean values of the water surface elevation and water velocity. In Taiwan, for practical purposes, engineers use a deterministic number for the water surface elevation and water velocity to calculate the hydrodynamic loading as the demand. In such cases, the uncertainty of floods is usually ignored. To take such uncertainty into consideration, the earlier reports (WRAMOEA, 2009, 2011a, 2011b) and the simulation results are used in the following calculation. Several reports (WRAMOEA, 2009, 2011a, 2011b) have recommended values of the water surface elevation and water velocity for engineers, and there is a noticeable variation among the suggested values. Thus, a Bayesian method is proposed to combine the indirect information (or information according to judgement) with additional or experimental data. The unknown parameter (i.e. the mean values of the water surface elevation and water velocity in this study) of a distribution is assumed to be a random variable. Available reports are assumed to be the indirect knowledge because they are generally not up to date, and simulation results are considered to be additional information. Based on the Bayesian approach, the posterior distribution of the target parameter (the mean values of the water surface elevation and water velocity) is described as follows

$$13. \quad f''(\theta) = \frac{P(\varepsilon|\theta)f'(\theta)}{\int_{-\infty}^{\infty} P(\varepsilon|\theta)f'(\theta)\mathrm{d}\theta}$$

where θ is the distribution parameter for the mean values of the water surface elevation and water velocity; ε denotes the outcomes of the HEC-RAS simulations; $P(\varepsilon|\theta)$ is the likelihood

of the simulation outcome ε assuming a given θ; $f'(\theta)$ is the prior probability derived from the existing reports; and $f''(\theta)$ is the posterior probability.

If the simulation outcome ε in Equation 13 is a set of values $x_1, x_2, \ldots, x_n$ representing a random sample from a population X with underlying density function $f_X(x)$, the posterior function described in Equation 13 can be revised as follows.

$$14. \quad f''(\theta) = \frac{\left[\prod_{i=1}^{n} f_X(x_i|\theta)\mathrm{d}x\right]f'(\theta)}{\int_{-\infty}^{\infty}\left[\prod_{i=1}^{n} f_X(x_i|\theta)\mathrm{d}x\right]f'(\theta)\mathrm{d}\theta} = kL(\theta)f'(\theta)$$

where k is the normalising constant and is expressed as

$$15. \quad k = \left\{\int_{-\infty}^{\infty}\left[\prod_{i=1}^{n} f_X(x_i|\theta)\mathrm{d}x\right]f'(\theta)\mathrm{d}\theta\right\}^{-1}$$

whereas $L(\theta)$ is the likelihood function and is calculated as

$$16. \quad L(\theta) = \prod_{i=1}^{n} f_X(x_i|\theta)\mathrm{d}x$$

If X is a Gaussian population (verified in Section 4.1.1) with a known STD (σ), the likelihood function for the target parameter μ (the mean values of the water surface elevation and water velocity) is

$$17. \quad \begin{aligned} L(\theta) &= \prod_{i=1}^{n} \frac{1}{\sqrt{2\pi}\sigma}\exp\left[-\frac{1}{2}\left(\frac{x_i-\mu}{\sigma}\right)^2\right] \\ &= \prod_{i=1}^{n} N_\mu(x_i,\sigma) = N_\mu\left(\bar{x}, \frac{\sigma}{\sqrt{n}}\right) \end{aligned}$$

where $N_\mu(x_i, \sigma)$ denotes the Gaussian density function of μ with mean value x_i and STD (σ); $\bar{x}$ is the sample mean. One of advantages of the Bayesian approach is that the prior information can be included in the estimation of parameter μ. Suppose that $f'(\mu)$ is $N(\mu', \sigma')$. The posterior probability in Equation 14 can be revised as shown below.

$$18. \quad \begin{aligned} f''(\mu) &= kL(\mu)f'(\mu) = kN_\mu\left(\bar{x}, \frac{\sigma}{\sqrt{n}}\right)N_\mu(\mu',\sigma') \\ &= N_\mu\left[\frac{\bar{x}(\sigma')^2 + \mu'(\sigma^2/n)}{(\sigma')^2 + (\sigma^2/n)}, \sqrt{\frac{(\sigma')^2(\sigma^2/n)}{(\sigma')^2 + (\sigma^2/n)}}\right] \end{aligned}$$

The Bayesian estimator for the target parameter is the mean value of the posterior function as described in Equation 19.

$$19. \quad \hat{\mu} = \frac{\bar{x}(\sigma')^2 + \mu'(\sigma^2/n)}{(\sigma')^2 + (\sigma^2/n)}$$

where $\hat{\mu}$ is the Bayesian estimator for the mean values or STDs of the water surface elevation and water velocity, σ' is the STD of the earlier reports, μ' is the mean value of the earlier reports, and $\bar{x}$ and σ are the mean and STD of samples from the HEC-RAS simulations, respectively. Note that due to the lack of prior information, the STD of the water surface elevation and water velocity is not updated by the Bayesian approach. Further discussion on this problem is provided later in Section 5.4.

4.3 Consideration of uncertainty in river geometry

The dynamic nature of rivers is usually ignored in a bridge design process. However, such characteristics may have significant impacts on bridge safety. For example, changes in runoff and sediment types may cause instability leading to river adjustments in the form of changes in channel shape, size, location or water velocity. Various definitions of river channel stability have been presented. For example, Richards (1987) described a stable channel as having constant average dimensions over a medium time frame (on the order of decades). Griffiths (1983) defined a stable channel as one in which channel dimensions of slope, width and depth remained balanced between erosion and sedimentation of channel beds and banks, input and output sediment discharge. Chorley and Kennedy (1971) described stability in terms of three types of equilibrium: (*a*) static; (*b*) steady-state; and (*c*) dynamic. Nevertheless, a stable river is often characterised by healthy, upright, woody vegetation, low banks with a flood plain and resilience to disturbances. Unstable channels can be a potential threat to a bridge, but they do not necessarily cause problems. For bridges, various channel instabilities can lead to channel bed degradation, channel widening and lateral migration.

A bridge might also collapse due to river channel instability. For example, the US Route 51 Bridge over the Hatchie River in Tennessee collapsed during a 3 year flood (FHWA, 2006). The collapse was caused by a lateral channel migration of 25·3 m over 13 years. The rate of lateral migration had increased dramatically following channel straightening to reduce the angle at which the channel approached the bridge. The example bridge illustrated in the present study is located in the Dajia River basin in central Taiwan. The geology of this basin is not in a well-engineered condition. After the occurrence of the 921 earthquake (magnitude 7·2, 1999), the situation became worse. For example, the geology became more vulnerable. More debris flows are found in the mountain area and more sediment in the catchment area. Two typhoons, Toraji (2001) and Mindulle (2004), struck this area followed by the 921 earthquake, resulting in a very special and atypical state in this basin: sediments are often found in the upstream and scour is occurring in the downstream. The Dajia River is in an unstable state, and this issue should be considered in any bridge safety evaluation. Six different geometries are collected, as shown in Figure 4. The variations in the channel bed profile and channel width are noticeable, indicating the instability of the Dajia River. To account for river geometry uncertainty,

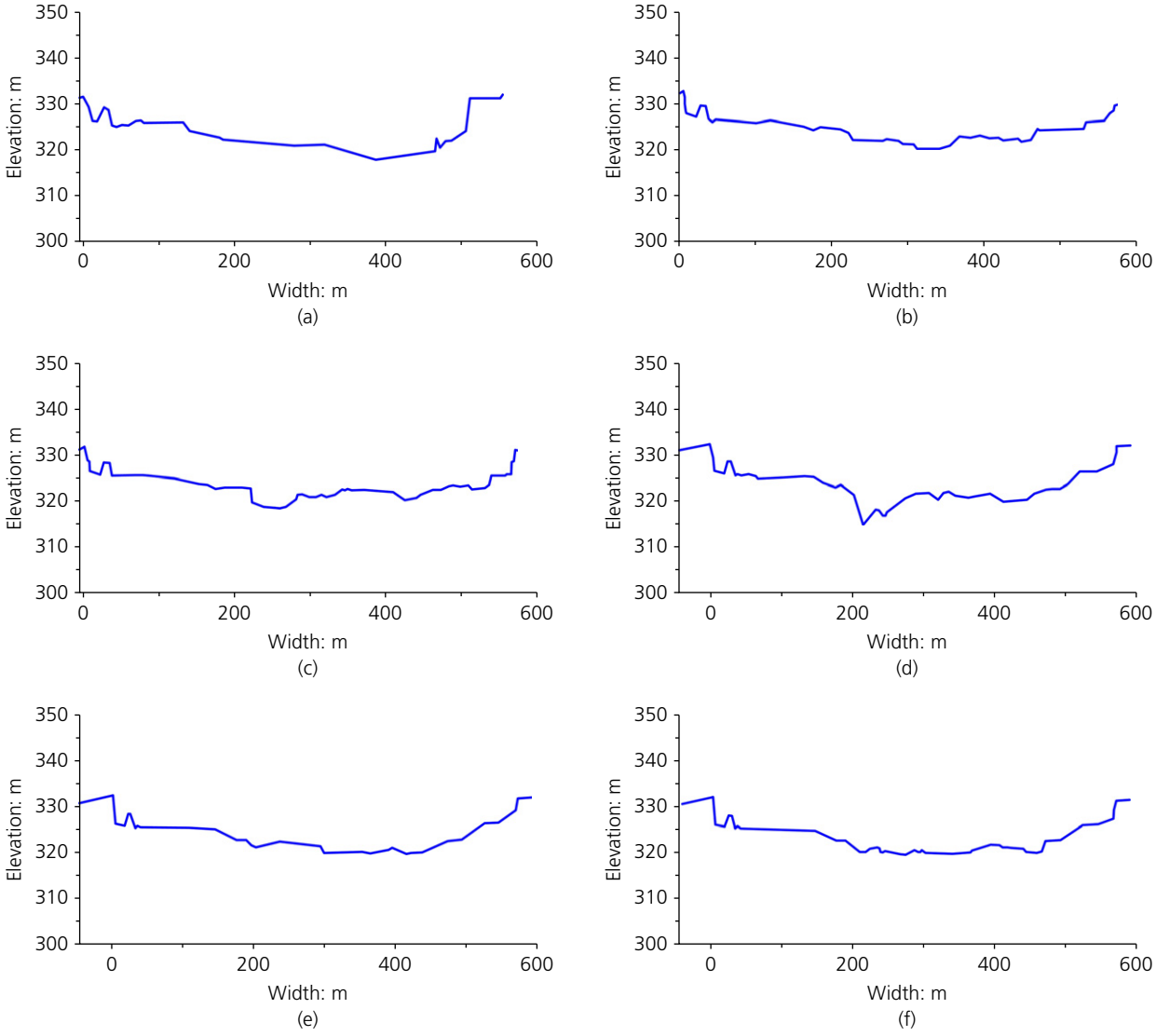

Figure 4. Six different river geometries used in the study: (a) 2000; (b) 2005; (c) 2008; (d) 2010; (e) 2011; (f) 2012

these six geometries are used in the proposed reliability safety evaluation.

5. Case study

This study uses MCS to calculate the bridge reliability during floods. The flowchart of the proposed approach is shown in Figure 1. The Tong-Shi Bridge (point D in Figure 5), located in the mid-stream of the Dajia River, is used to verify the proposed algorithm. The Tong-Shi Bridge is an important river bridge connecting the Dongshi district and the Shihgang district. Its entire length is 573 m with 22 spans; each span is approximately 26 m. The Tong-Shi Bridge has two piers in each substructure, as shown in Figure 6. The concrete strength is 28 MPa and 21 MPa for the bridge pier and pile, respectively. The steel bar used is SD280 for a diameter less than or equal to 16 mm, whereas SD420W is used for a diameter greater than 16 mm.

Figure 5. The Dajia River basin

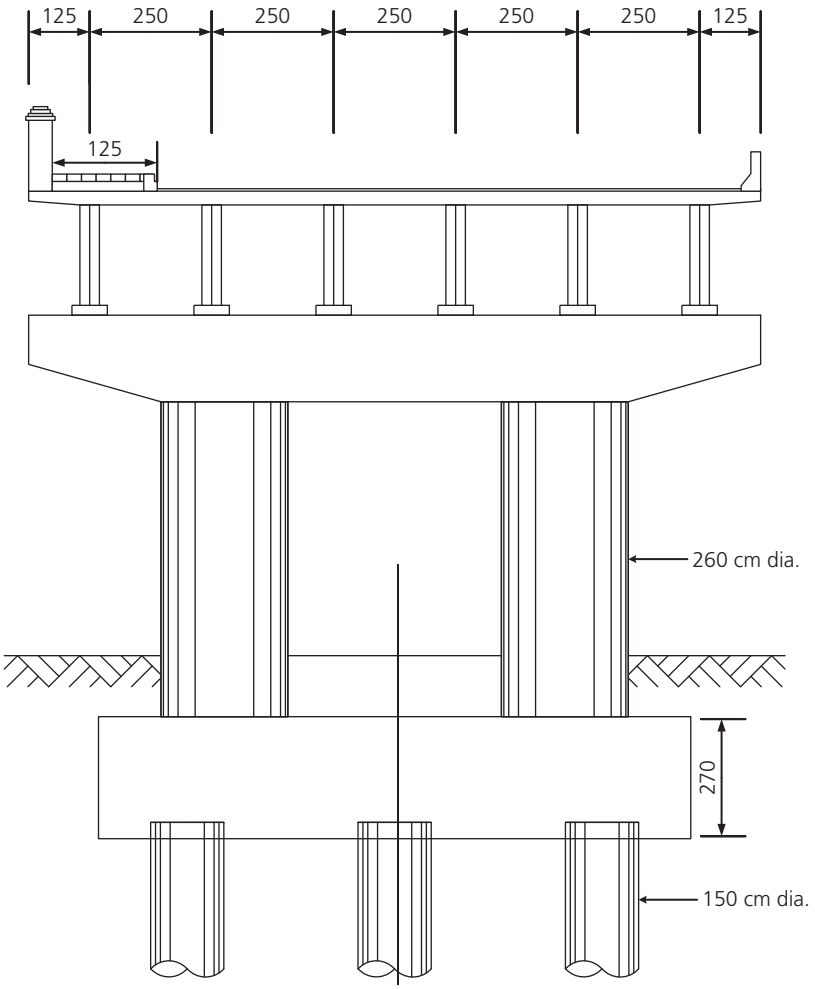

Figure 6. The typical foundation of Tong-Shi Bridge (unit: cm)

The Tong-Shi Bridge over the Dajia River is part of the No. 3 road that has two piers in each substructure. Several foundations were seriously damaged during the Chi-Chi earthquake (1999) and were reconstructed immediately afterwards.

5.1 Determination of the sample size for MCS

The MCS solution can be considered as a random variable. To provide a comprehensive description of the MCS solution, the coefficient of variation (COV) of the failure probability should be provided. It is widely accepted that the MCS solution is a binomial distribution, and the COV of a solution can be estimated as follows

$$20. \quad COV = \sqrt{\frac{1 - P_f}{nP_f}}$$

where P_f is the failure probability and n is the number of samples. A target COV of 10% is predefined. As a result, the required sample size of MCS ranges roughly from 1000 to 10 000 based on the failure probability for each considered year. Note that, for the current case study, the computational cost is in a reasonable range.

5.2 The random variables for the Tong-Shi Bridge

Based on the description in Section 4, the statistics of the considered random variables for the Tong-Shi Bridge are shown in Table 2. Note that most of the COVs are greater than 0·15, indicating that variations in these parameters are significant and should not be ignored. As expected, using multiple empirical equations causes the local scouring depth to have the highest COV. Although a more accurate prediction model for the scouring depth can be used to reduce the epistemic uncertainty, this topic is beyond the scope of the current study.

5.3 The HEC-RAS model for the Dajia River basin

Figure 5 displays the Dajia River basin (from point A to point B). Because the outflow discharge of the nearest dam in the upstream area dominates the variation in the water surface

Table 2. Statistics of the random variables for the Tong-Shi Bridge (2012)

Random variable	Mean	COV	pdf
Water velocity	6·07 m/s	0·29	Normal
Water surface elevation	6·77 m	0·16	Normal
Local scour depth	7·62 m	0·73	Normal
SPT-*N*	Provided in Section 4.1.3	Provided in Section 4.1.3	Uniform
Manning coefficient	0·033	0·22	Uniform

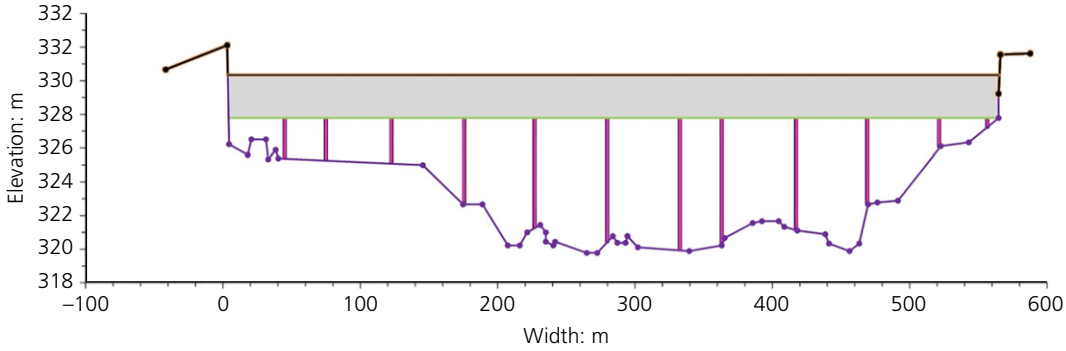

Figure 7. Example of an HEC-RAS river cross-section with bridge

level and velocity for the considered bridge, the designed HEC-RAS model includes only an area from the Ma-An dam to the sea shore, as shown in Figure 5 (from point C to point B). In the considered area, there are 98 river cross-sections, denoted as short cross-lines along B–D–C in Figure 5. Point C is the Ma-An dam, which is the nearest dam to the Tong-Shi Bridge (point D) in the upstream area. To build a better model, hydraulic structures such as bridges are included in the HEC-RAS model, as shown in Figure 7. There are two different types of motion for open-channel dynamics, one shallow and fast (supercritical flow) and the other deep, slow and in a low energy state (subcritical flow). For example, pools are often characterised as a subcritical flow due to the properties of deep water, slow flow, a surface slope that is near zero and low Froude numbers. Such characterisation can help engineers evaluate the potential for sediment entrainment and erosion along the channel boundary. However, it would be risky to characterise rivers into a fixed flow type because the same river may exhibit varying properties (e.g. irregular bottom slope of a river). Thus, a mixed flow condition was used in the HEC-RAS model. The water velocity and level for different flow conditions were compared, as displayed in Table 3. Note that the difference among the three models is insignificant.

5.4 Results and discussion

The reliability results for 2010 are displayed in Table 4. The serviceability is the dominant limit state. The foundation (e.g. the pile), by contrast, does not play an important role. A possible reason is that the Tong-Shi Bridge has just been completed as a retrofitted project and its pile capacity is properly ensured.

Table 3. Hydraulic measurements for the Tong-Shi Bridge under different conditions (2010)

	Stream surface elevation: m	Water velocity: m/s
Mixed	324·57	6·60
Subcritical	324·82	6·14
Supercritical	324·53	6·64

For example, the pile diameter in Taiwan often ranges from 0·4 m to 1·5 m. The pile diameter of the Tong-Shi Bridge is 1·5 m. Note that the pile used in the Tong-Shi Bridge has been well designed.

In the sensitivity analysis (Table 5), it is evident that the reliability of the bridge has a highly non-linear relationship with the design variables. For example, a 20% reduction in the pile diameter results in a 400% increase in the system failure probability. Similarly, a 40% increase in the scour depth leads to a 550% increase in the system failure probability. Table 5 also indicates that system reliability relies on the pile size significantly. For example, both soil capacity and pile structure have a serious problem when a pile size of 0·6 m is used in the Tong-Shi Bridge.

Table 6 shows reliabilities for different years, and a noticeable variation among them can be observed. Detailed discussion of these observations is provided below. Various river cross-sections were collected and used for the HEC-RAS simulations,

Table 4. System reliability of the Tong-Shi Bridge (for 2010)

Failure mode	Soil bearing	Soil pulling force	Pile shear strength	Pile axial strength	Serviceability	System
Failure probability	~0	~0	~0	~0	0·09	0·09

Table 5. Sensitivity of the failure probability

		Failure mode				
Factor	Change rate: %	Soil bearing	Soil pulling force	Pile shear strength	Pile axial strength	Serviceability
Pile	20[a]	~0	~0	~0	~0	0·3806
	60[b]	~0	0·2534	0·3178	~0	0·9846
Scour depth	40[c]	~0	~0	~0	~0	0·5252

[a]Pile diameter reduced from 1·5 m to 1·2 m
[b]Pile diameter reduced from 1·5 m to 0·6 m
[c]Scour depth increased from 7·62 m to 10·67 m

Table 6. Failure probability in six different years

Year	2000	2005	2008	2010	2011	2012
P_f	~0·00	0·03	~0·00	0·09	0·01	0·09

resulting in different water velocities and surface elevations, as shown in Table 7. Note that, in 2010, the average surface elevation had the highest value, and thus, 2010 was the most unreliable year. However, a higher surface elevation by itself is not sufficient to cause an unreliable bridge system. As shown in Table 7, the surface elevation and the water velocity in 2000 are similar to those in 2010. Unlike in 2010, however, in 2000, the structure appears to be the most reliable. Thus, the water surface elevation is an important but not a sufficient factor for bridge reliability. Reliability of a structure is often affected by the mean value and associated uncertainty (e.g. STD) of the performance function, as indicated in the definition of the reliability index shown in Equation 21.

$$21. \quad \beta = \frac{\mu_M}{\sigma_M}$$

where M indicates the performance function, μ is the mean value, σ is the STD and β is the reliability index. From Table 8, it is evident that a slight difference among the mean values (especially the velocity) is observed. However, a considerable difference in the STDs is found. A larger STD results in a smaller β, indicating a higher failure probability. This implies that a cross-section-induced variation in water velocity and surface elevation is a sufficient factor in bridge reliability. Note that not only the STDs, but also the mean values of the water velocity and surface elevation are affected by the cross-section. However, the mean values were updated using Bayesian theory with the official reports (Section 4.2), which resulted in a smaller variation compared to that of the STD. Apparently, more information reduces the variation in the random variables. Note that except for the simulated data, no other information about the variations of the water surface level and velocity could be found. This can be explained by the fact that most design processes in Taiwan use a deterministic approach (the mean value is the only parameter needed in a design process). Variation of the information is not an input parameter and is therefore not specified in the design documents.

6. Conclusions

Bridge safety evaluation is a challenging task. One of the reasons is that there are many uncertainties involved in the evaluation process. A probabilistic approach was proposed to account for uncertainties and evaluate bridge system reliability using MCS. Based on the current preliminary inspection items and literature, this study focused on the most influential factor, namely, the reliability of the target bridge structure. Random variables such as the water surface elevation, water velocity, local scour depth, wind load and soil property were considered in the hydraulic analysis. A system reliability evaluation was conducted in which five limit states were included. Comparing the proposed approach with the existing deterministic evaluation process, this study provided more detailed information for bridge safety. Some important conclusions are drawn below.

(*a*) To evaluate the uncertainties involved in bridge safety evaluation, a probabilistic analysis process must be adopted to provide more precise safety information.
(*b*) The maximum annual failure probability of the Tong-Shi Bridge over six different years was $1{\cdot}0 \times 10^{-3}$, which is roughly equal to the threshold value ($1{\cdot}00 \times 10^{-3}$) suggested by the International Organization for Standardization (ISO) (Davis-McDaniel *et al.*, 2013). The Tong-Shi Bridge was recently reconstructed based on the present code and is expected to have the ability to

Table 7. Stream velocities (Vel., m/s) and surface elevations (Sur., m) in six different years

	2000		2005		2008		2010		2011		2012	
Year	Vel.	Sur.	Vel.	Sur.	Vel.	Sur.	Vel.	Sur.	Vel.	Sur.	Vel.	Sur.
Mean	6·08	6·76	6·38	6·00	6·21	6·70	6·07	6·77	6·35	5·35	6·50	4·91
STD	0·59	0·92	0·89	0·69	0·68	0·93	1·77	1·06	0·75	0·62	0·81	0·50

Table 8. Variation of the mean and STD during six different years

	Mean of velocity	Mean of surface elevation	STD of velocity	STD of surface elevation
COV	0·03	0·13	0·49	0·27

withstand damage from flood hazard, which is consistent with the reliability calculation result in this study, indicating that the proposed procedure provides a reasonable reliability estimation.

(*c*) In the sensitivity analysis, it is confirmed that a system reliability analysis composed of multiple limit state functions should be adopted because the inactive performance function may become active in some conditions.

(*d*) The sampling approach was suggested because the performance functions were highly non-linear functions of random variables.

(*e*) The uncertainty in river cross-geometry has a significant impact on the bridge reliability and should be considered.

(*f*) Currently, the uncertainty in local scouring is comparatively high due to the limited knowledge. Improvements in empirical equations might enhance the accuracy of the reliability analysis results.

(*g*) If both prior and posterior information are available, a Bayesian approach is suggested to effectively reduce the variations in random variables.

Acknowledgement

This study was supported by the National Science Council of Taiwan under grant number NSC 103-2815-C-011-013-E. The support is gratefully acknowledged.

REFERENCES

Chang YL and Chou NS (1989) Chang's simple side pile analysis approach. *Sino-Geotech* **25**: 64–82.

Chorley RJ and Kennedy BA (1971) *Physical Geography: A Systems Approach*. Prentice-Hall, London, UK.

CPAMI (Construction and Planning Agency, Ministry of the Interior) (2001) *Building Foundation Design Specifications*. CPAMI, Taipei, Taiwan.

Davis-McDaniel C, Chowdhury M, Pang WC and Dey K (2013) Fault-tree model for risk assessment of bridge failure: case study for segmental box girder bridges. *Journal of Infrastructure Systems* **19(3)**: 326–334.

FHWA (Federal Highway Administration) (2006) *Assessing Stream Channel Stability at Bridges in Physiographic Regions*. FHWA, McLean, VA, USA, Publication No. FHWA-HRT-05-072.

Griffiths GA (1983) Stable-channel design in alluvial rivers. *Journal of Hydrology* **65(4)**: 259–270.

Johnson PA, Clopper PE, Zevenbergen LW and Lagasse PF (2015) Quantifying uncertainty and reliability in bridge scour estimations. *Journal of Hydraulic Engineering* **141(7)**: 04015013-1–04015013-9.

Liao KW, Lu HJ and Wang CY (2015) A probabilistic evaluation of pier-scour potential in the Gaoping River Basin of Taiwan. *Journal of Civil Engineering and Management* **21(5)**: 637–653.

Mander JB, Priestly MJN and Park R (1988) Theoretical stress–strain model for confined concrete. *Journal of Structural Engineering, ASCE* **114(8)**: 1804–1826.

MOTC (Ministry of Transportation and Communications) (2004) *Geological Report of Engineering Geological Prospecting*. MOTC, Taipei, Taiwan.

MOTC (2009) *The Bridge Design Specifications*. MOTC, Taipei, Taiwan.

Richards K (1987) *River Channels: Environment and Process*. Institute of British Geographers, Oxford, UK, Special Publications Series, 17.

Saydam D, Frangopol DM and Dong Y (2013) Assessment of risk using bridge element condition ratings. *Journal of Infrastructure Systems* **19(3)**: 252–265.

Sung YC, Liu KY, Su CK, Tsai IC and Chang KC (2005) A study on pushover analyses of reinforced concrete columns. *Journal of Structural Engineering and Mechanics* **21(1)**: 35–52.

WRAMOEA (Water Resources Agency, Ministry of Economic Affairs) (2009) *Study on River Bed Stability for the Reach Downstream of Ba-Pawn Dam in Dajia River*. WRAMOEA, Taipei, Taiwan.

WRAMOEA (2011a) *Study on River Bed Stability for the Reach Downstream of Shigang Dam in Dajia River*. WRAMOEA, Taipei, Taiwan.

WRAMOEA (2011b) *Regulation Master Plan of Dajia River*. WRAMOEA, Taipei, Taiwan.